

Study on the Effect of Premixed Gas Addition on the Anti-Blow-Off Performance of Jet Diffusion Flame

Makihito NISHIOKA, Kosuke MIYAZAKI, Hiroki TAKAYAMA, Akane UEMICHI

Department of Engineering Mechanics and Energy, University of Tsukuba

1-1-1 Tennodai, Tsukuba, Ibaraki, Japan

1 Introduction

Jet diffusion flames have been widely used for a variety of practical applications because of their extensive range of safety and high controllability. However, when low-grade fuels such as biogas are used, they are apt to be lifted or blown off because of their weakness of reactions. So it is desirable to develop new techniques to improve the anti-blow-off performance of jet diffusion flames of such fuels, since effective utilization of them as an energy resource is now becoming more and more necessary.

The stabilization mechanism of jet diffusion flames is rather complicated and largely changes depending on the width of burner rim or injection velocities. In the case of a thin burner rim, Takahashi et al. [1,2] showed the existence of “reaction kernel” and investigated its role in stabilizing the flame base. According to their studies, a reaction kernel is formed mainly by the reaction between H radical and O₂, the former of which comes from the downstream diffusion flame by back diffusion, while the latter comes from the surrounding air also by diffusion through the gap between the flame base and the burner rim.

Recently we conceived an idea of addition of small amount of premixed gas at the flame base for enhancing the reaction kernel, and applied the idea for the stabilization of “pseudo biogas” (methane diluted with nitrogen) that cannot be stabilized on an ordinary injector at all because of the weakness of reactivity. Since the intrusion of O₂ from the surrounding is essential for forming a reaction kernel of an ordinary diffusion flame, we think that artificially added O₂ help the kernel grow strongly. In this study, we performed experiments of jet diffusion flame of pseudo biogas using a coaxial double-tube burner, in which small amount of premixed gas is injected between the tubes, and measured the blow off limit of the injection velocity of main fuel jet or coflowing air. Additionally, detailed-kinetics numerical simulations were also conducted for investigating the phenomena occurring around the reaction kernel formed on the coaxial double-tube burner.

2 Experimental Setup and Experimental/Numerical Conditions

Figures 1 (a) and 1 (b) show the schematics of the coaxial double-tube burner used in this study, and the closeup of the rims of two coaxial injector tubes, respectively. The coaxial double-tube injector made of stainless steel was set in a coflowing air supply system composed of a settling chamber, straw bundle and a glass chimney. Fig. 1 (b) also shows the diameters of the injector tubes. Two types of outer tubes with different diameters were used, while the inner injector tube diameter was fixed to 5 mm i.d. The

thicknesses of all injector tubes are 0.5 mm. Table 1 shows the inner and outer diameters of all injector tubes used in this study. The distance between the exit planes of the inner tube and the outer tube, Δz , is variable. Fuel and additional premixed gas are injected from the inner tube and the gap between the two coaxial tubes, respectively. Air is introduced into the settling chamber and after rectification by the straw bundle it is injected uniformly in the glass chimney of 600 mm i.d. coaxially set with the injector.

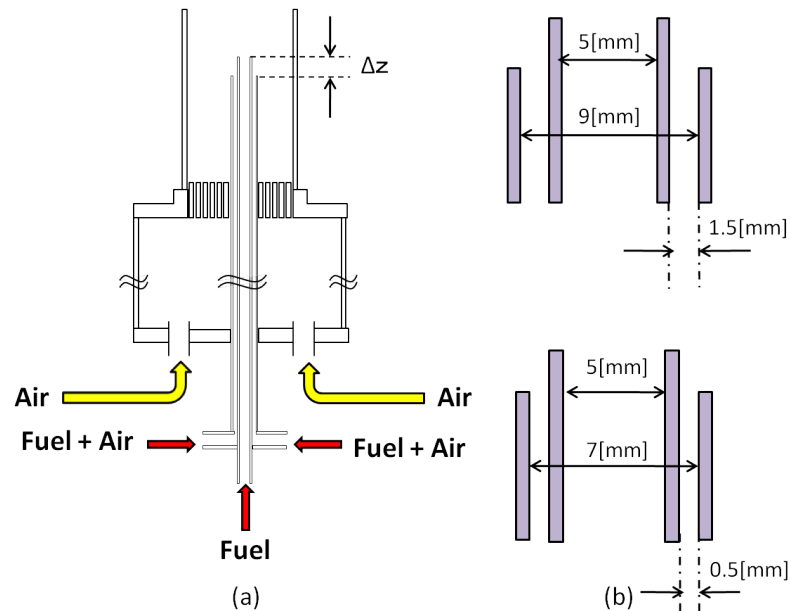


Fig. 1. Schematics of the burner: (a) the entire burner and (b) the closeup views of the tube rims.



Fig. 2. Direct photograph of the diffusion flame base. The conditions are $\Delta z = 12$ mm, $U_f = 300$ cm/s, $U_p = 20$ cm/s ($L_p = 7.068$ cm³/s), $U_a = 10$ cm/s and $D_{outer} = 10$ mm.

Table 2 shows the experimental conditions. In this study, “pseudo low-grade biogas” composed of 30% methane and 70% nitrogen was used for the main fuel jet and also for the fuel component of the additional premixed gas. This fuel mixture is too weak to form a diffusion flame on an ordinary injection tube at all even for a very small injection velocity. Equivalence ratio of the additional premixed gas was set 4.0. Figure 2 shows the direct photograph of the diffusion flame base with premixed gas being injected from the gap between the two coaxial tubes. In this case the distance Δz is 12 mm, which is the maximum value used in this study. As shown in Table 2, the injection velocity of additional premixed gas, U_p , were changed for the four values of the distance Δz . Under these conditions, we conducted experiments

for examining the following two types of blow off limit:

Case I: Blow off by coflowing air,

Case II: Blow off by main fuel jet.

In the Case I, the coflowing air velocity was gradually increased with the main fuel jet velocity fixed at 300 cm/s, and when the flame was blown off we defined the velocity as the blow off limit by the coflowing air. In the Case II, on the other hand, the main fuel jet flow velocity was gradually increased with the coflowing air velocity fixed at 10 cm/s, and when the flame was blown off we defined the fuel velocity as the blow off limit by main fuel jet. The injection velocity conditions of fuel and air for each case are shown in Table 3.

The numerical code used in this study is a detailed-kinetics code that has been developed by Nishioka, the details of which were described in Ref. 3. The adopted kinetics scheme is so-called C1 chemistry extracted from GRI-mech3.0 [4].

Table 1. Inner and outer diameters of the injector tubes.

	Inner Diameter	Outer diameter
Inner tube	$d_{\text{inner}}=5\text{mm}$	$d_{\text{outer}}=6\text{mm}$
Outer tube 1	$D_{\text{inner}}=7\text{mm}$	$D_{\text{outer}}=8\text{mm}$
Outer tube 2	$D_{\text{inner}}=9\text{mm}$	$D_{\text{outer}}=10\text{mm}$

Table 2. Experimental conditions.

Fuel	CH ₄ 30% + N ₂ 70% (by volume ratio)
Oxidizer	Air
Equivalence ratio of additional premixed gas	4.0
Distance between the exit planes of the inner tube and the outer tube: Δz	6, 8, 10, 12 mm
Additional premixed gas velocity: U_p	5 ~ 100 cm/s

Table 3. Injection velocity conditions for the cases I and II.

	Case I	Case II
Main fuel jet velocity: U_f	300 cm/s	0 cm/s ~
Coflowing air velocity: U_a	0 cm/s ~	10 cm/s

3 Results and Discussions

3.1 Experimental Results of the Blow Off Limits

Figures 3 and 4 show the results of the experiments. Fig. 3 shows the blow off limit by coflowing air, while Fig. 4 shows the one by main fuel jet. In these figures the abscissas are the flow rate of additional premixed gas, L_p , while the ordinates are the critical coflowing air velocity and the critical main fuel jet velocity, respectively. It must be noted that for both cases the critical U_a and U_f are both zero without addition of premixed gas ($L_p = U_p = 0$), i.e., the flame cannot be stabilized on the burner at all.

It is seen in Fig. 3 that the largest limit of blow off by coflowing air was attained at the condition of $\Delta z = 12$ mm and the premixed gas flow rate $L_p = 10.60$ cm³/s ($U_p = 30$ cm/s) for the Outer tube 2 ($D_{\text{outer}} = 10$ mm). When L_p is less than about 4 cm³/s the blow off limit increases monotonically with L_p , but it turns to decrease or to be almost constant for the further increase of L_p . There is a considerable discrepancy between the cases with Outer tube 1 and 2, but the basic response of the blow off limit to L_p is almost the same. It is noted that Δz does not affect the limit much for L_p less than about 4 cm³/s, but it starts to cause the difference of the limit as L_p is increased further.

In the case of blow off by main fuel jet, on the other hand, there exists a large difference of the blow off limit between the cases with Outer tube 1 and 2. When Outer tube 2 ($D_{outer}=10$ mm) is used the response of the limit to L_p is similar to that of the blow off by coflowing air, with the effect of Δz being relatively small. When Outer tube 1 ($D_{outer}=8$ mm) is used, on the other hand, the response differs largely between the cases of $\Delta z = 6, 8$ mm and the cases of $\Delta z = 10, 12$ mm. In the latter cases the highest blow off limit is attained at $L_p = 7.147$ cm³/s ($U_p = 70$ cm/s) for $\Delta z = 12$ mm. It must be noted that the flame is not blown off up to the highest fuel jet velocity of $U_f = 13$ m/s.

In both cases of blow off by coflowing air and by main fuel jet, it was found that $\Delta z = 12$ mm cases show the highest anti-blow-off performance among the four values of Δz . In Fig. 2, in which $\Delta z = 12$ mm, it is seen that the flame base exists near the inner tube rim and a long flameless zone is formed between the rims of two coaxial tubes. So it is natural to anticipate that there is some phenomenon playing a key role in stabilizing a jet diffusion flame.

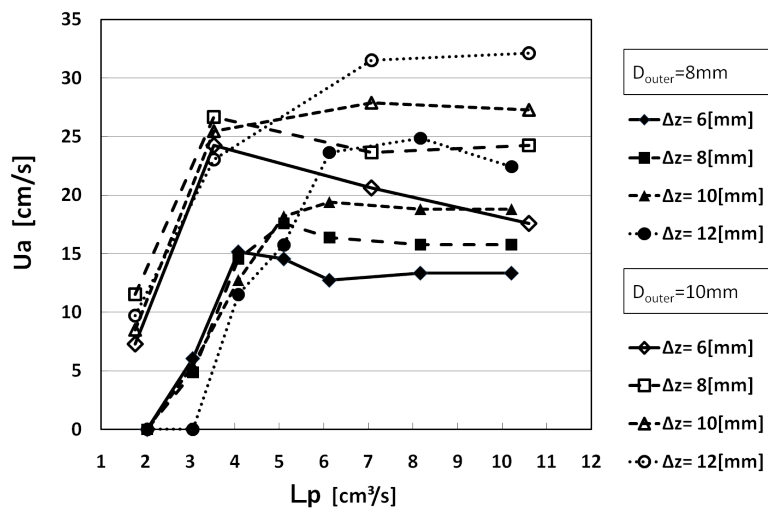


Fig.3. Critical coflowing air velocity U_a as a function of the premixed gas flow rate L_p .

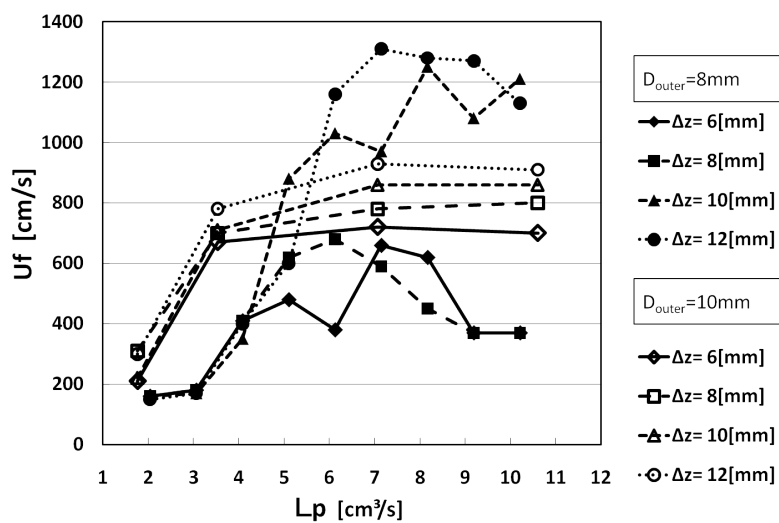


Fig.4. Critical main fuel jet velocity U_f as a function of the premixed gas flow rate L_p .

3.2 Numerical Results

To examine the phenomena occurring within the abovementioned long flameless zone between the rims of two coaxial tubes, we performed an axisymmetric, two-dimensional numerical calculations with detailed kinetics for the case of $\Delta z = 12$ mm, $U_f = 300$ cm/s, $U_p = 20$ cm/s, $U_a = 10$ cm/s and $D_{\text{outer}} = 10$ mm, which are just the same as the flame shown in Fig. 2.

Figure 5 shows the numerical result. Here, (a) and (b) respectively show the distributions of the heat release rate and the mole fraction of methane. In Fig. 5 (a), it is seen that the reaction kernel at the base of the diffusion flame is extended outwardly forming a kind of “reaction zone wing”. In Fig. 5 (b), on the other hand, it is seen that the concentration of methane, which has been originally contained in the additional premixed gas, decreases from the exit of the outer tube to the downstream. That is, the methane in the premixed gas diffuses outwardly forming a premixed gas with the surrounding air. It is noted that the configuration of the reaction zone shown in Fig. 5 (a) is quite similar to that of the blue flame in Fig. 2.

Considering the concentration gradient formed in the long flameless zone as shown in Fig. 5 (b), we expect that the reaction zone wing in Fig. 5 (a) is a kind of premixed flame that is formed in the same manner as that of a tribrachial flame. In a tribrachial flame, a lean premixed flame wing and a rich premixed flame wing are formed in the lean side and the rich side of a diffusion flame surface, respectively. In the case of the flame in Fig. 5 (a), the wing looks similar to the lean side branch of a tribrachial flame, which suggests that a lean-side half wing of a tribrachial flame is formed in a peculiar concentration field formed between the fuel flow and the additional premixed gas flow divided by an inner injector tube. Since the wing obviously is a premixed flame, it has a local burning velocity that can balance the local flow velocity. Thus, the mechanism of improving the anti-blow-off performance by addition of premixed gas is thought to be closely related to the phenomenon of tribrachial flame.

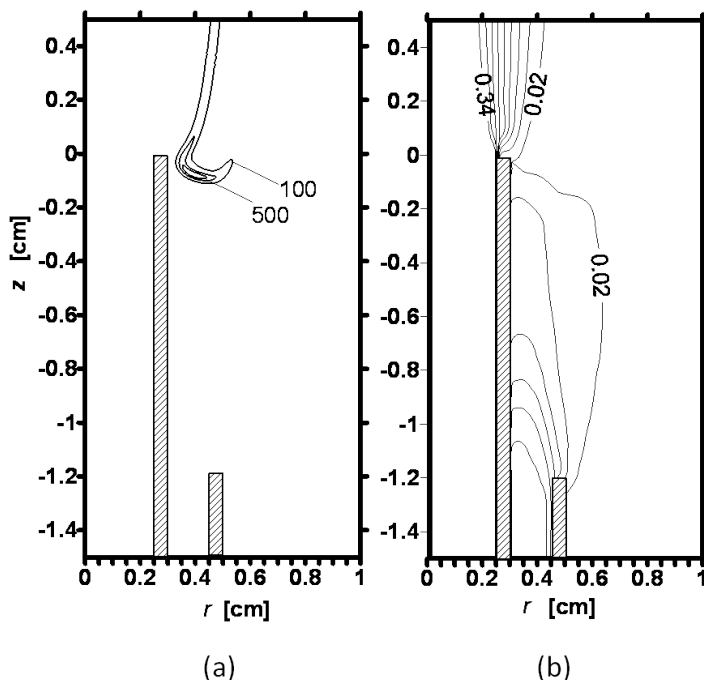


Figure 5. Calculation results. (a) Distributions of heat release rate. Unit is $\text{J}/(\text{cm}^3\text{-s})$. (b) Distribution of methane mole fraction. $\Delta z = 12$ mm, $U_f = 300$ cm/s, $U_p = 20$ cm/s, $U_a = 10$ cm/s, $D_{\text{outer}} = 10$ mm.

References

- [1] F. Takahashi, W.J. Schmoll, V. Katta, *Proceedings of the Combustion Institute* 27 (1998), 675.
- [2] F. Takahashi, V. Katta, *Proceedings of the Combustion Institute* 28 (2000), 2071.
- [3] M. Nishioka, Y. Ishigami, H. Horii, Y. Umeda, Y. Nakamura, *Combustion and Flame* 147 (2006), 93.
- [4] G.P. Smith, D.M. Golden, M. Frenklach, N.W. Moriarty, B. Eiteneer, M. Goldenberg, C.T. Bowman, R.K. Hanson, S. Song, W.C. Gardiner Jr., V.V. Lissianski, Z. Qin, <http://www.me.berkeley.edu/gri-mech/>.
- [5] B.E. Lee, S.H. Chung, *Combustion and Flame* 109 (1997), 163.